Assembly Mechanism of *Dictyostelium* Myosin II: Regulation by K^+, Mg^{2+}, and Actin Filaments†

Rohit K. Mahajan‡ and Joel D. Pardee*

Department of Cell Biology and Anatomy, Cornell University Medical College, New York, New York 10021

Received July 31, 1996⊗

ABSTRACT: Regulated assembly of myosin II in *Dictyostelium discoideum* amoebae partially controls the orderly formation of contractile structures during cytokinesis and cell migration. Kinetic and structural analyses show that *Dictyostelium* myosin II assembles by a sequential process of slow nucleation and controlled growth that differs in rate and mechanism from other conventional myosins. Nuclei form by an ordered progression from myosin monomers to parallel dimers to 0.43 μm long antiparallel tetramers. Lateral addition of dimers to bipolar tetramers completes the assembly of short (0.45 μm) blunt-ended thick filaments. Myosin heads are not staggered along the length of tapered thick filaments as in skeletal muscle, nor are bipolar minifilaments formed as in *Acanthamoeba*. The overall assembly reaction incorporating both nucleation and growth could be kinetically characterized by a second-order rate constant ($k_{obs,N+G}$) of 1.85×10^4 M^{-1} s^{-1}. Individual rate constants obtained for nucleation, $k_{obs,N} = 4.5 \times 10^3$ M^{-1} s^{-1}, and growth, $k_{obs,G} = 2.5 \times 10^4$ M^{-1} s^{-1}, showed *Dictyostelium* myosin II to be the slowest assembling myosin analyzed to date. Nucleation and growth stages were independently regulated by Mg^{2+}, K^+, and actin filaments. Increasing concentrations of K^+ from 50 to 150 mM specifically inhibited lateral growth of dimers off nuclei. Intracellular concentrations of Mg^{2+} (1 mM) accelerated nucleation but maintained distinct nucleation and growth phase kinetics. Networks of actin filaments also accelerated the nucleation stage of assembly, mechanistically accounting for spontaneous formation of actomyosin contractile fibers via myosin assembly (Mahajan et al., 1989). The distinct assembly mechanism and regulation utilized by *Dictyostelium* myosin II demonstrates that myosins from smooth muscle, striated muscle, and two types of amoebae form unique thick filaments by different pathways.

The dynamic behavior of *Dictyostelium* myosin II during cytokinesis and cell migration [Yumura & Fukui, 1985; Kitanishi-Yumura & Fukui, 1989; Nachmias et al., 1989; Aguardo-Velasco & Kuczmarski, 1993; reviewed in Fukui and Yumura (1986) and Warrick and Spudich (1987)] has spurred an interest in the cytoplasmic regulation of thick filament formation. In *Dictyostelium*, cell migration is accompanied by transposition of myosin II structures from random cortical locations to the trailing cell edge where a contractile band is formed (Yumura & Fukui, 1985; Nachmias et al., 1989). Dividing cells also demonstrate a similar repositioning of myosin II to the cleavage furrow during late anaphase of mitosis (Yumura & Fukui, 1985; Kitanishi-Yumura & Fukui, 1989). Consequently, how myosin is assembled and translocated in the cytoplasm is of interest for determining how the cytoskeleton controls cell motility and cytokinesis. We have presented evidence that actin filaments can directly mediate myosin assembly by providing polymer networks upon which bipolar thick filaments form (Mahajan et al., 1989; Applegate & Pardee, 1992). Tail phosphorylation of *Dictyostelium* myosin II prevents assembly (Kuczmarski & Spudich, 1980) and induces translocation through the cytoskeleton (Egelhoff et al., 1993). Still, how cytoplasmic actin networks and myosin reversibly form contractile fibers at specific locations remains unclear.

Kinetic assembly mechanisms have now been reported for skeletal muscle, smooth muscle, and *Acanthamoeba* myosin II. Skeletal muscle myosin polymerizes into 0.6−1.6 μm tapered bipolar thick filaments containing up to 400 myosin molecules [Pepe & Drucker, 1979; Pinset-Harstrom & Truffy, 1979; Reisler et al., 1980; Saad et al., 1986; reviewed in Cross et al. (1991a), Herbert and Carlson (1971), Koretz (1982), and Pepe (1982)]. Tapered bipolar thick filaments form by staggered addition of parallel dimers to antiparallel bare zone nuclei [Harrington & Rogers, 1984; Pepe, 1982; reviewed in Cross et al. (1991a)]. In striated muscle, thick filament length is dictated by decreasing affinity of dimers for the growing thick filament ends (Davis, 1986). Smooth muscle myosin forms both 0.6 μm bipolar and 6 μm side-polar filaments under these conditions (Craig & Megerman, 1977; Cross et al., 1991a,b; Hinssen et al., 1978; Kendrick-Jones et al., 1982; Megerman & Lowey, 1981; Small, & Sobieszek, 1980; Trybus, 1991). Non-muscle myosin from *Acanthamoeba* shows a markedly different structure and assembly mechanism from muscle myosins. *Acanthamoeba* myosin II assembles within 70 ms by initially forming antiparallel dimers that laterally associate into 0.3 μm long minifilaments containing 8−16 myosin molecules (Pollard, 1982; Sinard & Pollard, 1990; Sinard et al., 1989). Myosin II from other sources can also form minifilament type structures, but does so under non-physiologic conditions that are selective for each myosin (Kuczmarski et al., 1988;

† This work was supported by NIH Grant GM32458, BRSG Grant S07 RR05396, an Andrew Mellon Distinguished Scientist/Teacher Award, and an Irma T. Hirschl/Monique Weill Career Scientist Award to J.D.P.

* Corresponding author. Tel: (212) 746-6153. FAX: (212) 746-8175.

‡ Current address: Department of Cell Biology, The Scripps Research Institute, 10666 N. Torrey Pines Road, La Jolla, CA 92037.

⊗ Abstract published in *Advance ACS Abstracts,* October 15, 1996.

S0006-2960(96)01898-3 CCC: $12.00

Pollard, 1982; Reisler et al., 1980, 1986; Sinard & Pollard, 1989; Trybus, 1991; Trybus & Lowey, 1987). Characterization of mammalian non-muscle myosins indicates assembly features of both smooth and skeletal muscle myosin (Cross et al., 1991b; Trybus & Lowey, 1987).

Dictyostelium myosin II assumes a variety of structures depending on the ionic envirionment, myosin phosphorylation state, and mode of assembly (Kuczmarski et al., 1987; Pasternak et al., 1989). Equilibrium mixtures of parallel dimers and antiparallel tetramers co-exist at low ionic strength (0−10 mM KCl). Phosphorylation near the carboxy terminal [Collins et al., 1982; Kuczmarski et al., 1988; reviewed in Korn and Hammer (1988) and Warrick and Spudich (1987)] induces looping of the myosin rod that prevents assembly under physiologic salt conditions (Kuczmarski & Spudich, 1980; Kuczmarski et al., 1987; Pasternak et al., 1989) and engenders translocation in the cytoplasm (Egelhoff et al., 1993). Comprehending how these various forms are orchestrated in the cytoplasm requires a knowledge of the primary assembly pathway for *Dictyostelium* myosin II. We report here on the assembly mechanism that slowly forms the short bipolar myosin filaments detected in the *Dictyostelium* cell cortex (Fukui & Yumura, 1986; Yumura & Fukui, 1985; Kitanishi-Yumura & Fukui, 1989; Nachmias et al., 1989). Sequential association of monomers to parallel dimers to bipolar tetramers is followed by lateral binding of dimers onto tetramers to create thick filaments. The highly controlled rate of *Dictyostelium* myosin II assembly is governed by intracellular concentrations of K^+, Mg^{2+}, and actin filaments. Mg^{2+} and F-actin promote initiation of the reaction, while K^+ determines the rate of thick filament growth by inhibiting additions to nuclei.

MATERIALS AND METHODS

Cell Culture. *D. discoideum* strain Ax-3 were grown in axenic culture with HL-5 medium (Loomis, 1971; Spudich, 1982). For protein purifications, cells were harvested by centrifugation at 700*g* for 6−8 min when cell density reached an OD_{660} of 0.8−1.0. Approximately 60−80 g of cells was obtained from 12 L of media.

Dictyostelium Myosin II Purification. Cytoplasmic actin and myosin II were separated on a 2.5 × 90 cm A-15M (Bio-Rad) gel filtration column following the original procedure of Clarke and Spudich (1974). Myosin- and actin-containing peaks were eluted at 20 mL/h and identified by SDS−polyacrylamide gel electrophoresis (Figure 1, lanes c and d). A modification of the Clarke and Spudich procedure was subsequently devised to obtain high yields of homogenous *Dictyostelium* myosin II and actin. Pooled A-15M myosin (90−120 mL; Figure 1, lane c) was dialyzed overnight against Thick Filament Buffer (Clarke & Spudich, 1974) (10 mM Tris-maleate, pH 6.5, 100 mM KCl, 1 mM DTT, 0.005% NaN_3), and the resulting thick filaments collected by centrifugation at 17000*g* for 30 min. Because a significant proportion of assembly-competent myosin remained unassembled, the assembly supernatant was concentrated 10-fold with Aquacide III (CalBioChem) at 4 °C, dialyzed against Thick Filament Buffer, and re-centrifuged. Thick filament pellets were combined, homogenized in 5−10 mL of Dissociation Buffer (10 mM Tris-HCl, pH 7.5, 0.5 M KCl, 1 mM DTT, 1 mM EDTA, 0.005% NaN_3; Clarke & Spudich, 1974) and dialyzed 15−20 h at 4 °C. Dissociated myosin was clarified for 30 min at 17000*g* and stored on ice. *Dictyostelium* myosin II isolated by this method has been shown to contain RNA that affects the association properties of thick filaments (Stewart & Spudich, 1979). Stock myosin was treated with 50 μg of pancreatic RNase/mL, Type III (Sigma), for 4 h at room temperature, dialyzed overnight against Dissociation Buffer, and clarified at 17000*g* for 30 min (Figure 1, lane e). The resulting 260/280 absorbance ratio of 0.8−1.0 indicated thorough removal of contaminating RNA. Significantly enhanced yields of approximately 21 mg of electrophoretically pure myosin composed of a 210 000-dalton heavy chain complexed with 18 000- and 16 000-dalton light chains were routinely obtained from 100 g of cells by this method. Final myosin concentration was approximately 6 mg/mL as determined by spectrophotometry $E_{280}^{0.1\%} = 0.52$; MW = 540 000; Clarke & Spudich, 1974).

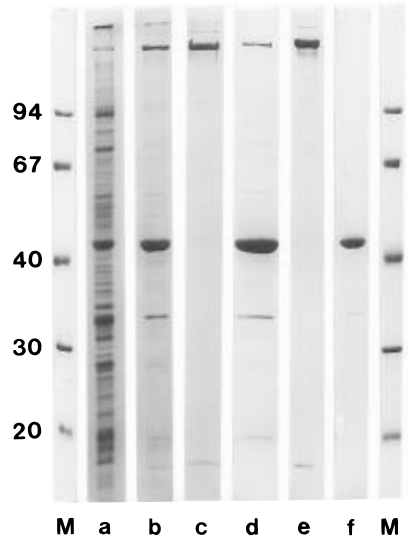

FIGURE 1: Co-purification of *Dictyostelium* myosin II and actin. SDS−PAGE of purification fractions. (a) Clarified cell lysate; (b) actin, myosin precipitate; (c) myosin pool from A-15M gel filtration column; (d) actin pool from A-15M gel filtration column; (e) RNase-treated myosin final product (5 μg). Purified myosin contained a 210 000-dalton heavy chain, an 18 000-dalton light chain, and a 16 000-dalton light chain. On the 10% acrylamide gels shown, the 16 000-dalton light chain co-migrates with the dye front and is not shown. (f) Actin final product (5 μg). Contaminating 30 kDa actin bundling protein was removed by recycling in the presence of Ca^{2+}. (M) Molecular weight markers; phosphorylase B (94 kDa), bovine serum albumin (67 kDa), ovalbumin (40 kDa), catalase (30 kDa), and soybean trypsin inhibitor (20 kDa).

Actin Purification. The A-15M column actin pool (100 mL) was purified to remove contaminating myosin and 30 kDa actin bundling protein (Figure 1, lane d) (Fechheimer & Taylor, 1984; Johns et al., 1988). Actin was dialyzed overnight against F-Buffer (2 mM triethanolamine, pH 7.0, 50 mM KCl, 1 mM DTT, 0.2 mM EGTA, 0.25 mM $MgCl_2$, 0.2 mM ATP, 0.005% NaN_3), and F-actin sedimented at 150000*g* for 90 min. F-actin pellets were disassembled in 10 mL of G-Buffer (4 mM Tris-HCl, pH 7.5, 0.2 mM DTT, 0.2 mM ATP, 25 μM $MgCl_2$, 1 mM EGTA, and 0.005% NaN_3) by overnight dialysis. G-actin was clarified by centrifugation at 150000*g* for 90 min, polymerized on ice in the presence of Ca^{2+} by sequential additions with mixing of ATP to 1 mM (from a pH 7.0 stock solution), $CaCl_2$ to 2 mM, KCl to 50 mM, and $MgCl_2$ to 1 mM. The sample was incubated with ATP and $CaCl_2$ for 5 min before addition of

KCl and $MgCl_2$. After assembly for 1 h on ice, filaments were sedimented at 150000*g* for 90 min, rinsed, homogenized in 5 mL of F-Buffer, and dialyzed overnight against F-Buffer. Purified F-actin (Figure 1, lane f) was stored on ice. By UV spectra ($E_{280}^{0.1\%} = 1.08$), approximately 20 mg of purified *Dictyostelium* F-actin was obtained per 100 g of cells. Actin was recycled prior to each experiment. F-actin (2 mg/mL) was disassembled by dialysis against G-Buffer, clarified at 150000*g* for 90 min at 4 °C and reassembled with 1 mM ATP, 50 mM KCl, and 1 mM $MgCl_2$ by sequential additions from stock solutions.

Assembly Assays. Myosin assembly kinetics were followed by turbidometric assays using a stopped-flow apparatus with a mixing time of approximately 20 ms (SFA-II, HiTech Scientific). Samples were mixed by injection into a 1 cm pathlength quartz cuvette in a Perkin Elmer Lambda 3B spectrophotometer and monitored at 300 nm. For assembly experiments in a specified experimental buffer, stock monomeric myosin at 6−10 mg/mL in Dissociation Buffer was initially dialyzed against the experimental buffer containing 0.5 M KCl to maintain myosin dissociation. Dialyzed stock was centrifuged at 100000*g* to remove residual myosin aggregates, and the myosin monomer concentration was adjusted so that a 1:10 dilution would yield the final desired myosin concentration. For example, myosin used for assembly in DdM Buffer was first equilibrated against 10 mM imidazole, pH 6.5, 1 mM DTT, and 0.5 M KCl. Assembly was initiated by a rapid 1:10 dilution into 10 mM imidazole, pH 6.5, 1 mM DTT, 1.11 mM $MgCl_2$, 1.11 mM ATP to obtain the final DdM assembly buffer condition (10 mM imidazole, pH 6.5, 1 mM DTT, 1 mM $MgCl_2$, 50 mM KCl, 1 mM ATP). By this method, constant myosin monomer and solvent compositions were obtained in the final mix. Increases in optical density at 300 nm due to turbidity were continously recorded during mixing and throughout assembly. Because the stopped-flow mixing apparatus employed is not quantitative for assembly experiments exceeding 120 s due to slow leakage of myosin into the cuvette, long-duration assembly measurements were initiated by manual dilution. In these cases, a 15−20 s interval between initial mixing and recording of optical density occurred.

Turbidity (τ) is linearly proportional to the Rayleigh ratio for scattered light at any given angle as defined by the relationship

$$\tau = -\ln(I/I_0) = K'R(\theta_s)$$

where I = incident light at 300 nm, I_0 is transmitted light through a 1 cm cuvette, $R(\theta_s)$ is the Rayleigh light scattering ratio at angle θ, and K' is the appropriate constant for angle θ (Marshall, 1978). Total solute turbidity is also defined by the concentration [c] and weight-averaged molecular weight, M_w, of the scattering species, making quantification of myosin assembly into thick filaments possible by the linear relationship

$$\tau = \sum R(\theta_s) = K[c]M_w$$

where K is the constant for light scattering summed over 180° minus scatter at 0°. Turbidity, instead of 90° light scattering, was used to follow myosin assembly, because unlike angle scattering, total scattered light is minimally affected by the shape of the scattering species.

The extent of myosin assembly during rate measurements was quantitated from specific molar turbidities established separately for thick filaments and dimers. To obtain a specific molar turbidity for myosin dimers, aliquots of assembly mixtures were fixed with 6% glutaraldehyde at 20 s of assembly, turbidities taken, and the sample analyzed by negative staining electron microscopy to assay for the presence of myosin monomers and dimers. For 2.2×10^{-7} M myosin assembled in DdM buffer, complete conversion of monomers to dimers occurred by 10 s of assembly (see Figures 4a and 5b), and an average ratio of dimer/tetramer of 60/1 was observed after 30 s of assembly (data not shown). A specific molar turbidity of

$$\epsilon_{300}^{M} = 4.2 \times 10^3 \text{ OD M}^{-1} \text{ cm}^{-1}$$

$$= \frac{(\tau_{dimer} - \tau_{monomer}) \text{ OD cm}^{-1}}{[\text{myosin}]}$$

was obtained from the turbidities of salt-dissociated monomers in DdM buffer containing 0.5 M KCl, and from 20 s assembly mixtures containing >98% dimers. To define the relationship between turbidity and myosin dimer formation, the theoretical treatment of Berne (1974) for light scattering of long rods was invoked. In general, turbidity increases linearly with polymerization when the polymer thickness is significantly less than the length of the shortest polymer and the wavelength of incident light. The criteria for linearity are described by the Q_0 function, defined as $(2\pi\upsilon/\lambda)(L)2^{-0.5}$, where Q_0 is dependent on polymer length (L) and wavelength (λ). The Berne relationship between polymer length and turbidity shows a linear rise for Q_0 = values exceeding 2.5. In our myosin assembly system, a Q_0 value of 3.0 at λ = 300 nm is obtained for a myosin monomer length of 200 nm, and a Q_0 value of 3.2 is obtained for parallel dimers of 215 nm containing a 15 nm stagger. Both Q_0 values fall on the linear portion of the turbidity vs Q_0 curve for light scattering of long rods (Berne, 1974). Consequently, monomer to parallel dimer transitions in which length increases from 200 to 215 nm fall on the linear portion of the turbidity curve (Berne, 1974), making turbidity increases directly proportional to the concentration of dimeric units in solution. In this transition, the apparent exponential dependence of turbidity on length is 3.3 for both monomers and dimers.

The specific molar turbidity for fully formed *Dictyostelium* myosin II thick filaments was calculated from the turbidities of glutaraldehyde fixed filaments after 10 min of assembly in DdM buffer and from monomers in DdM buffer + 0.5 M KCl.

$$\epsilon_{300}^{M} = 2.5 \times 10^5 \text{ OD M}^{-1} \text{ cm}^{-1}$$

$$= \frac{(\tau_{\text{thick filaments}} - \tau_{monomer}) \text{ OD cm}^{-1}}{[\text{myosin}]}$$

Electron microscopy of *Dictyostelium* myosin II assembled in DdM buffer showed blunt-ended thick filaments measuring 0.45 μm long and 0.2 μm thick. Elongation of thick

filaments off of bipolar tetramers did not occur, and the final filament thickness was small compared to its length. Consequently, the turbidity signal observed during growth of thick filaments is derived from elongation of dimers to antiparallel tetramers. Incorporation of dimer subunits into thick filaments during growth is turbidometrically equivalent to dimer to tetramer conversion. On the basis of the Berne calculation, the turbidity increases accompanying tetramer or thick filament formation are linearly dependent on removal of dimers from solution. Q_0 values change from 3.2 for dimers to approximately 6.7 for thick filaments (Berne, 1974). The linear relationship between thick filament growth and turbidity was experimentally confirmed by sedimentation assays taken during the growth phase of assembly. Samples fixed at 50% of maximum turbidity showed only thick filaments together with dimers, and sedimentation of these mixtures at 100000*g* quantitatively removed thick filaments which comprised 48−55% of the total myosin. Half-maximal turbidity therefore corresponded to a $t_{1/2}$ for assembly of dimers into thick filaments. Molar turbidity of thick filaments measured 2.5×10^5 M^{-1} cm^{-1} compared to 4.2×10^3 M^{-1} cm^{-1} for dimers, or 99% of total turbidity. This is in agreement with the 94% contribution to turbidity by filament myosin observed during assembly of skeletal muscle myosin (Davis, 1981b). Combined theoretical considerations and the independent experimental techniques of molar turbidity, EM, and sedimentation analysis defined a linear increase in turbidity which paralleled thick filament formation. In *Dictyostelium* assembly curves, rates extrapolated from the linear portion of the assembly curve during growth fit a second-order kinetic scheme over the 10-fold range of myosin concentrations tested.

Rate constants for assembly were obtained from both extrapolated initial rates (R_i) in stopped-flow experiments of 120 s duration, as well as from overall assembly half-times ($t_{1/2}$) obtained from manual dilution assembly experiments carried out for 30 min. An association rate constant (k_{obs}) for assembly was calculated from initial changes extrapolated from light-scattering curves using the rate law and the determination of a second-order rate dependence on myosin concentration,

$$k_{obs} = \frac{R_{initial}}{[myosin]^2}$$

An overall apparent rate constant was also derived from the half-time of assembly, using the relationship

$$t_{1/2} = {k_{obs}}^{-1}[My_{t_{1/2}}]^{-1}$$

for second-order reactions (Gutfreund, 1972; Marshall, 1978), where $[My_{t_{1/2}}]$ is the concentration of unassembled myosin at $t_{1/2}$.

Buffers. Assembly was analyzed under a variety of buffer conditions and salt concentrations. The buffer of choice for measuring kinetics of *Dictyostelium* myosin II was 10 mM imidazole, pH 6.5, 1 mM DTT, 1 mM $MgCl_2$, 50 mM KCl, 1 mM ATP or 1 mM AMPPNP (DdM Buffer), which reflected current information on cytoplasmic concentrations of K^+ (Aeckerle et al., 1985), Mg^{2+} (J. Pardee, unpublished data), and H_3O^+ (Fechheimer et al., 1986) in *Dictyostelium*. Assembly rate and final thick filament morphology comparisons were made to other selected buffers cited in the literature for *Acanthamoeba* myosin II (AcM-a Buffer; 10 mM imidazole, pH 6.8, 20 mM KCl) (AcM-b Buffer; 10 mM imidazole, pH 6.8, 20 mM KCl, 10 mM $MgCl_2$) (Pollard, 1982), rabbit skeletal muscle myosin (SkM Buffer; 5 mM bicine, pH 8.1, 150 mM KCl) (Davis, 1981a), and smooth muscle myosin (SmM Buffer; 25 mM imidazole, pH 7.0, 150 mM NaCl, 10 mM $MgCl_2$, 0.2 mM EGTA, 0.25 mM DTT) (Craig et al., 1983). The final *Dictyostelium* myosin concentration in assembly assays ranged from 2×10^{-8} to 1.5×10^{-6} M in concentration dependence studies and was 2.2×10^{-7} M in all other experiments. Kinetics of chicken skeletal muscle and *Dictyostelium* myosin assembly was compared between 2.2×10^{-7} M *Dictyostelium* myosin and 2.7×10^{-7} M muscle myosin in both DdM and SkM Buffers. Effects of F-actin on *Dictyostelium* myosin assembly were carried out in F-Buffer containing 2 μM F-actin, 100 mM KCl, 1 mM $MgCl_2$, and 1 mM ATP or AMPPNP, pH 7.0.

Electron Microscopy. Assembling myosin was rapidly fixed by adding reaction mixture aliquots to freshly prepared 30% glutaraldehyde to achieve a final concentration of 6%. To examine the aggregation state of unassembled myosin, stock myosin in 0.5 M KCl was diluted directly into DdM Buffer containing 6% glutaraldehyde. Rapid fixation was evidenced by examination of intermediate species obtained during sequential time points of assembly. Samples fixed at 0−5 s contained only myosin dimers. More advanced states of assembly (tetramers and thick filaments) were not present, providing evidence for rapid and stoichiometric trapping of intermediates on a seconds time scale. Skeletal muscle myosin thick filaments have been successfully fixed by this procedure without attendant aggregation or disassembly (Davis, 1985), and myosin dimers were established as skeletal myosin assembly intermediates by 30 min fixation in glutaraldehyde added to pressure-depolymerized thick filaments (Davis et al., 1982). 10 μL aliquots of the fixed reaction mix were subjected to negative staining electron microscopy. Samples fixed for a minimum of 30 min were applied to nitrocellulose, carbon-coated grids for 1 min and stained with 1% uranyl acetate clarified through a 0.22 μm filter. Several drops of stain were washed over the grids and the final drop allowed to set for 1 min. Stained grids were subsequently blotted on edge with filter paper, air dried, and viewed in a JEOL 100CXII electron microscope (JEOL, Peabody, MA) at 80 kV accelerating voltage.

RESULTS

Assembly Kinetics

Reaction Order. The dependence of assembly half-time ($t_{1/2}$) on increasing myosin concentration was used to establish the apparent overall reaction order for *Dictyostelium* myosin II assembly. Continuous turbidometric tracings were used to define $t_{1/2}$ by interpolation to 50% of the maximum OD_{300nm} obtained for complete assembly (Figure 2a). To determine if the apparent half-time obtained from turbidometry accurately reflected 50% myosin incorporation into thick filaments, samples at $t_{1/2}$ were immediately fixed with glutaraldehyde and analyzed for unassembled myosin after centrifugation at 100000*g* (see Methods). Half-time mixtures for myosin concentrations from 10^{-6} to 10^{-7} M contained 48−55% unassembled myosin, verifying that turbidometry was a reliable and linear measure of myosin assembly at $t_{1/2}$. Similar measurements at 25% and 75% of maximum

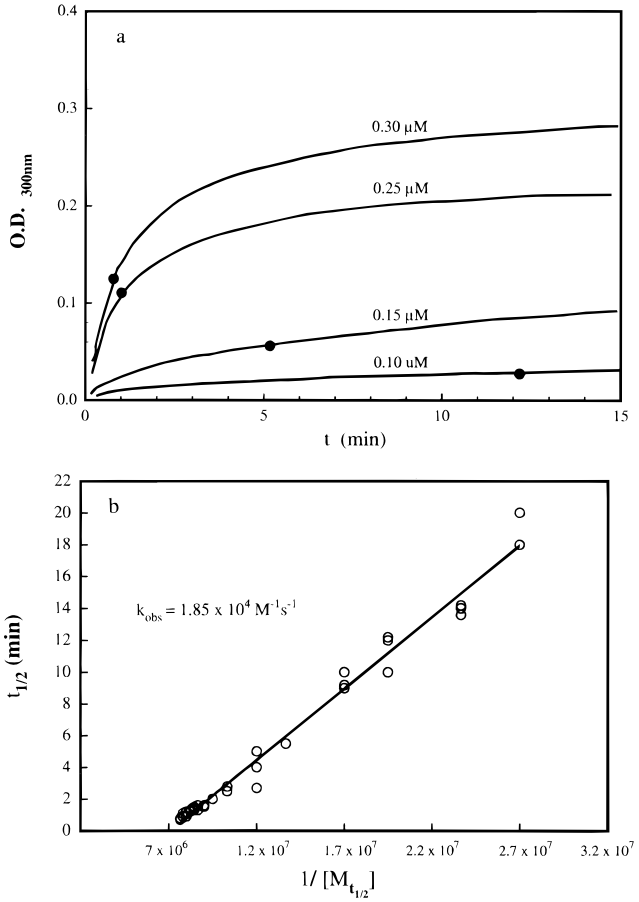

FIGURE 2: Assembly kinetics and reaction order. (a) Continuous turbidometric tracings of assembling myosin. Representative curves for selected concentrations are shown. (●) Represents the half-time, $t_{1/2}$, for the overall assembly curve. (b) Dependence of assembly half-time on unassembled myosin concentration at $t_{1/2}$. A linear fit to the second-order rate equation indicated a second-order assembly reaction with an overall rate constant (k_{obs}) of 1.85 $\times$ 10^4 M^{-1} s^{-1}.

turbidity indicated 20−24% and 74−81% myosin sedimentation, respectively (data not shown). Plots of $t_{1/2}$ versus 1/[My$_{t_{1/2}}$] over a 75-fold range of myosin concentrations produced a linear regression fit to the second-order rate equation, $t_{1/2} = (1/k_{app})(1/[My_{t_{1/2}}])$ (Figure 2b) (Gutfreund, 1972; Marshall, 1978). An overall on-rate constant (k_{obs}) of 1.85 $\times$ 10^4 M^{-1} s^{-1} (Figure 2b) was calculated from the plot slope, making this the slowest association rate obtained for myosin from any source (see Discussion).

Biphasic Assembly. To clearly evaluate early assembly events, kinetics were analyzed within 1 s of assembly initiation by stopped-flow mixing. Stopped-flow analysis showed that *Dictyostelium* myosin II followed a distinctly biphasic assembly time course (Figure 3a). Lag phase kinetics of this type have been ascribed to polymerization reactions that proceed by a mechanism of slow nucleation followed by rapid growth off nuclei (Oosawa & Kasai, 1971). A plot of log R_i versus log[myosin] showed two rate dependencies (Figure 3b). At low myosin concentrations (<1.5 $\times$ 10^{-7} M), R_i was highly dependent on initial myosin concentration, consistent with a rate-limiting nucleation step. A forward rate constant for nucleation ($k_{obs,N}$) of (4.5 $\pm$ 0.7) $\times$ 10^3 M^{-1} s^{-1} was calculated from the initial rate dependence of the lag phase on myosin concentration. At high initial myosin concentrations, assembly rates were dictated

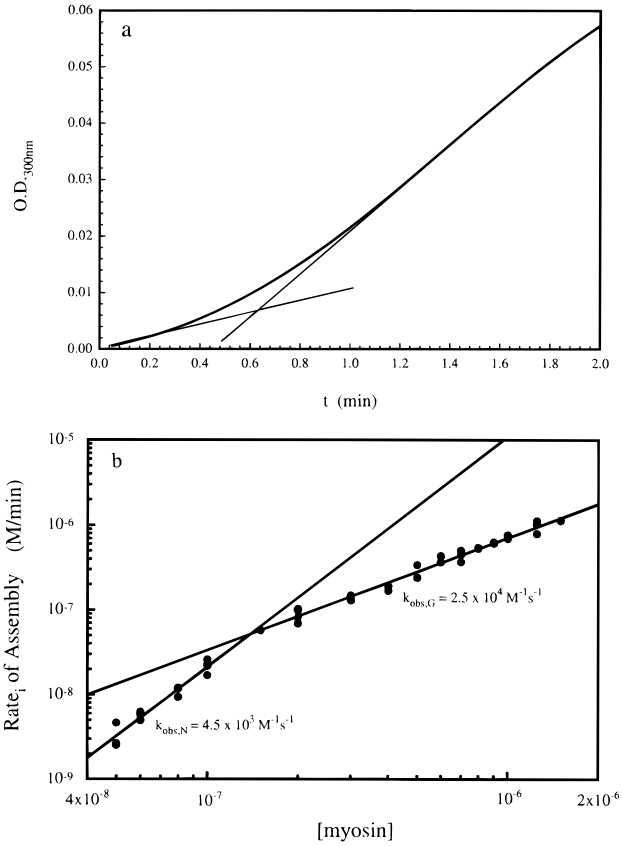

FIGURE 3: Detection of lag phase kinetics during *Dictyostelium* myosin II assembly. (a) Light scattering assembly curve at 2 $\times$ 10^{-7} M myosin. A distinct initial lag phase is detected. (b) Log−log plot of initial rate versus myosin concentration. Nonlinear regression analysis produced a bimodal linear fit showing slower initial nucleation kinetics coupled to a more rapid growth phase.

by growth phase equilibria. Initial growth phase rates defined a $k_{obs,G}$ of (2.5 $\pm$ 1.1) $\times$ 10^4 M^{-1} s^{-1}, slightly faster than the value calculated from the overall assembly half-time (1.85 $\times$ 10^4 M^{-1} s^{-1}), which includes the slower nucleation step of assembly. Overall kinetics derive from a relatively slow nucleation phase followed by more rapid growth. The deliberate assembly pace was not entirely due to nucleation, but also stemmed from the relatively slow growth of thick filaments from nuclei compared to skeletal muscle myosin (k_{obs} = 3.3 $\times$ 10^5 M^{-1} s^{-1}; Davis, 1981b) or *Acanthamoeba* myosin II (k_{obs} > 10^8 M^{-1} s^{-1}; Sinard & Pollard, 1990). On the basis of the reported rate constants, *Dictyostelium* myosin II assembles approximately 18 times slower than skeletal muscle (Davis, 1981b) and 5000 times more slowly than *Acanthamoeba* myosin II (Sinard & Pollard, 1990). Slow but detectable rates of assembly were obtained at 5 $\times$ 10^{-8} M myosin (27 μg/mL) and 2 $\times$ 10^{-8} M myosin (11 μg/mL). The critical concentration for assembly was therefore kinetically defined at <11 μg/mL, confirming previous observations of a negligible critical concentration for *Dictyostelium* myosin II by equilibrium sedimentation (Kuczmarski et al., 1987). Assembly rates in DdM Buffer were identical in the presence of 1 mM AMPPNP, ATP, or ADP (data not shown), indicating no nucleotide dependence for thick filament formation.

Filament Structures

Assembly Intermediates. Because of the relatively slow formation of *Dictyostelium* myosin II thick filaments, it was

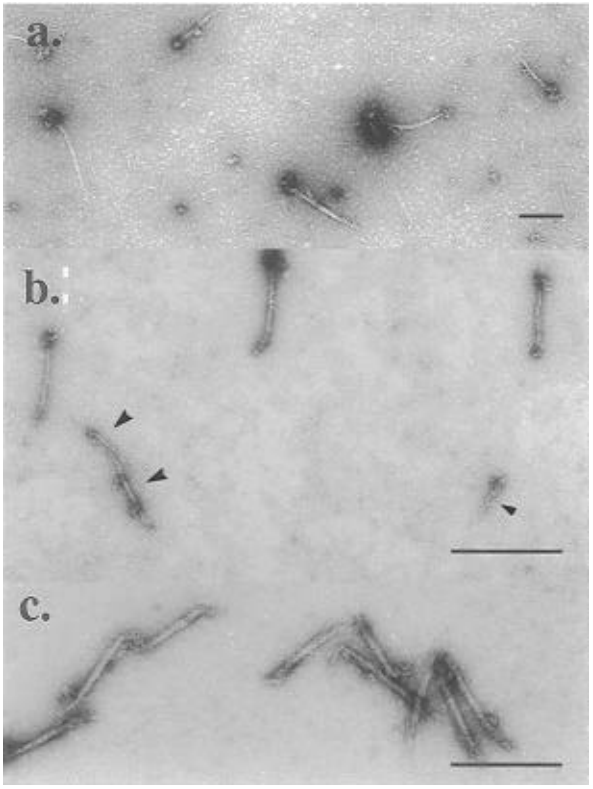

FIGURE 4: Assembling *Dictyostelium* myosin II. Representative electron microscopy fields of myosin assembled in DdM Buffer. (a) Parallel dimers after 10s of assembly. Bar, 0.1 μm. (b) Dimers (arrowheads) and bipolar tetramers at 20 s of assembly. Bar, 0.5 μm. (c) Thick filaments after 120 s of assembly. Bar, 0.5 μm.

possible to directly visualize assembly intermediates after fixation with glutaraldehyde. Low magnification survey micrographs of myosin assembly intermediates are shown during the nucleation and growth phases of assembly (Figure 4). Since low concentrations of myosin (2.2×10^{-7} M) were necessary in these experiments to slow the reaction and trap intermediates, EM fields contained few myosin molecules. Consequently, intermediates were also examined at high magnification to determine structure and extent of assembly (Figure 5). Samples taken before assembly (in 0.5 M KCl) and immediately after initiating assembly contained myosin monomers (Figure 5, 0−5 s). The rod portion of negatively stained monomers measured 180 nm in length and approximately 5.7 nm in width, consistent with previously established dimensions of *Dictyostelium* myosin (Kuczmarski et al., 1987; Pasternak et al., 1989). Tail portions exhibited helical twists (Figure 5, 0−5 s, arrows). Samples fixed at 10 s of assembly showed complete conversion of monomers into dimers (Figure 4a and Figure 5, 5−10 s). Dimers averaged 13 nm in width and contained aligned tail regions approximately 175 nm long. Dimer tail alignment was staggered by approximately 10% with 15−20 nm of tail extending past its paired partner (Figure 5, 5−10 s, arrowheads). Tail stagger has been previously observed by rotary shadowing in equilibrium dimer mixtures (Hodge et al., 1992; Kuczmarski et al., 1987; Pasternak et al., 1989). Assembling myosin fixed at 20 s, corresponding to a late stage of nucleation, contained dimers and antiparallel tetramers measuring 14 nm in width and 430 nm in overall length (Figure 4b and Figure 5, 10−20 s). This stage marked the first appearance of a bipolar arrangement during assembly and correlated with the end of the lag phase. Bipolar thick filaments measuring approximately 0.45 μm in length were formed by 2 min of assembly (Figure 4c and Figure 5, 120 s). While overall length remained constant, filament thickness varied with Mg^{2+} concentration. In DdM Buffer containing 1 mM Mg^{2+} filaments measured approximately 25 nm in diameter (Figure 4c), while DdM Buffer with 10 mM Mg^{2+} produced 34 nm diameter filaments (Figure 5, 120 s). Assuming closest parallel packing of myosin tails, each thick filament was calculated to contain a maximum of 72 myosin molecules when formed in 10 mM Mg^{2+}. At no stage of assembly did intermediates or thick filaments show elongation by successive stagger of subunits as has been observed in *Acanthamoeba* myosin minifilaments and skeletal muscle myosin thick filaments.

On the basis of the time course of visualized intermediates, assembly occurs by three association steps. Monomers initially associate to form parallel dimers. Dimer tails bind in opposing orientation to form an antiparallel tetramer which comprises the bare zone of the assembling thick filament. We propose that lateral addition of dimers to antiparallel tetramer nuclei completes the thick filament. In this scheme, overall assembly follows the reaction pathway below:

$$(1)\ \mathrm{M} + \mathrm{M} = \mathrm{D}, \quad r_1 = k_1[\mathrm{M}]^2 - k_{-1}$$

$$(2)\ \mathrm{D} + \mathrm{D} = \mathrm{T}, \quad r_2 = k_2[\mathrm{D}]^2 - k_{-2} \text{ and}$$
$$k_{\mathrm{obs,N}} = 4.5 \times 10^3\ \mathrm{M}^{-1}\ \mathrm{s}^{-1}$$

$$(3)\ n\mathrm{D} + \mathrm{T} = \mathrm{TD}_n$$
$$= \mathrm{F}_{n+2}, \quad r_3 = k_3[\mathrm{D}][\mathrm{T}] - k_{-3} \text{ and}$$
$$k_{\mathrm{obs,G}} = 2.5 \times 10^4\ \mathrm{M}^{-1}\ \mathrm{s}^{-1}$$

where M represents myosin monomer, D is parallel dimer, T is antiparallel tetramer, TD_n is tetramer−dimer complex containing 1 tetramer with n dimers, and F is the thick filament containing $n + 2$ dimers. Steps 1 and 2 constitute nucleation and step 3 represents growth of thick filaments by lateral association of dimers onto tetramer nuclei.

Assembly Regulation

Buffer Effects on Myosin Assembly. Thick filament morphology and assembly have been shown to be highly sensitive to pH, divalent cations, and ionic strength (Atkinson & Stewart, 1992; Cross et al., 1991a,b; Davis, 1988; Faruqi et al., 1993; Harrington & Rogers, 1984; Hodge et al., 1992; Koretz, 1982; Korn & Hammer, 1988; Pepe, 1982; Trybus, 1991). To compare regulation of *Dictyostelium* myosin II assembly within the family of myosins, assembly kinetics were determined in a variety of buffer systems cited in the literature to characterize muscle and non-muscle myosins. Buffer systems used for *Acanthamoeba* myosin II (AcM-a and AcM-b Buffers), skeletal muscle myosin (SkM Buffer), and smooth muscle myosin (SmM Buffer) had remarkably different effects on *Dictyostelium* myosin II assembly (Figure 6). Rates were fastest in AcM-a and AcM-b Buffers. A shortened lag phase of 10−15 s was observed in these low ionic strength buffers (20 mM KCl). Electron microscopy showed extensive aggregation of thick filaments, accounting for elevated turbidity of assembled myosin. In contrast, SkM and SmM Buffers containing 150 mM K^+ or Na^+ substantially inhibited the overall rate of *Dictyostelium* myosin II

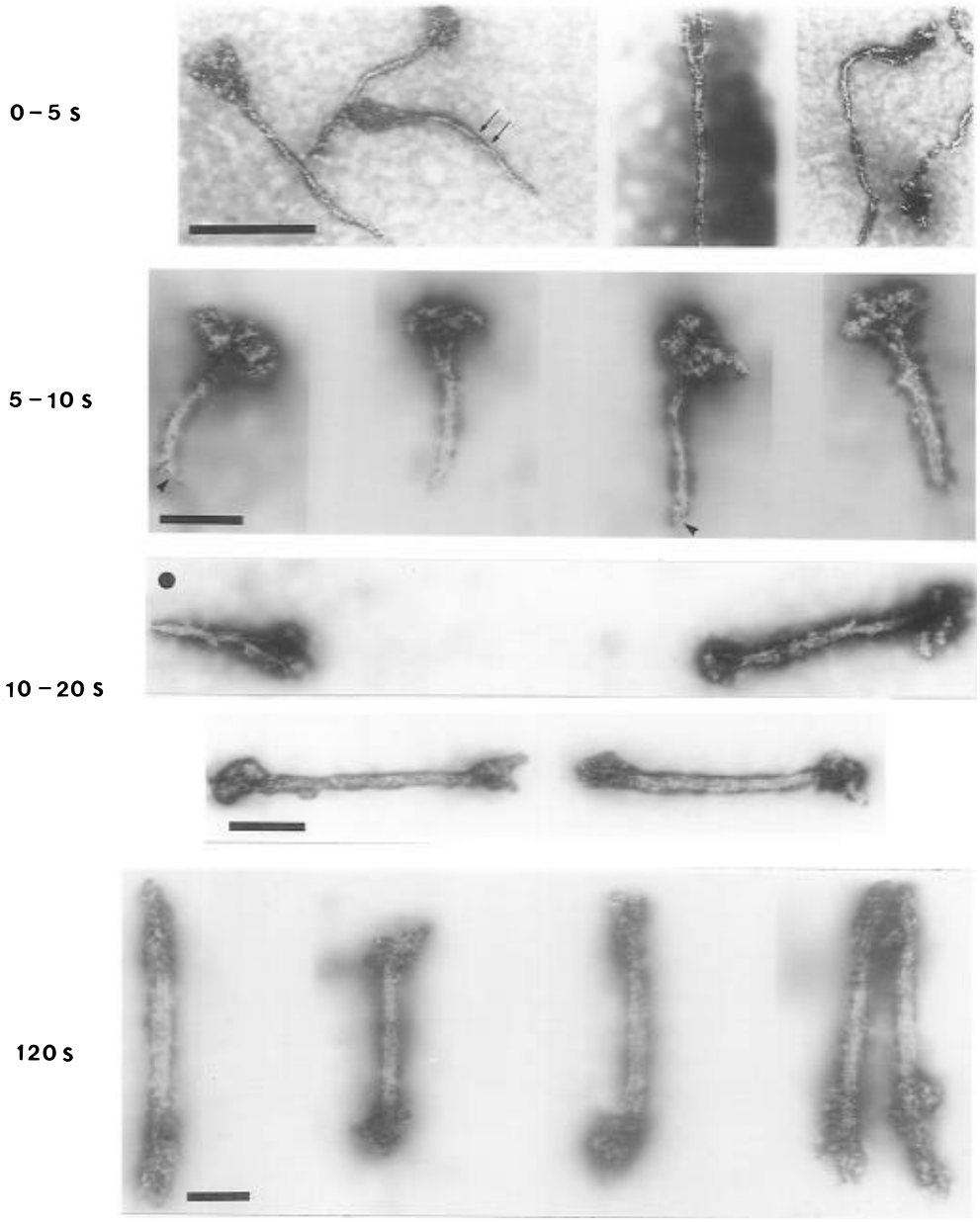

FIGURE 5: *Dictyostelium* myosin II assembly intermediates. High-magnification electron microscopy of myosin assembly intermediates. (0−5 s) High salt myosin monomers before assembly composed of two heavy chains in helical array (arrows). (5−10 s) Association of myosin into parallel dimers within 10 s of initiation of assembly. Panel shows samples fixed at 5 s post-initiation. Negatively stained dimers demonstrated staggered tail overlap (arrowheads). (10−20 s) Formation of antiparallel myosin tetramers. Mixtures of parallel dimers and bipolar tetramers characterized this stage of assembly. (120 s) Mature *Dictyostelium* myosin II thick filaments formed in 50 mM KCl, 10 mM Mg^{2+}, pH 6.5. (Bars, 0.1 μm.)

assembly compared to DdM Buffer. Na^+ had a stronger inhibitory effect than K^+, causing much slower assembly in SmM Buffer (150 mM Na^+, 10 mM Mg^{2+}) than in SkM Buffer (150 mM K^+, 0 Mg^{2+}). Assembly rates were not significantly altered in DdM, SkM, or SmM Buffers over a pH range from 6.5 to 8.0 (not shown). The rate of assembly nucleation was not significantly altered by any buffer (Figure 6b), predicting that monovalent ions specifically inhibited growth phase equilibria.

Inhibitory Effects of KCl. Because physiologic concentrations of monovalent ions produced significant inhibitory effects, stages of thick filament formation sensitive to K^+ were identified by increasing K^+ concentrations in DdM buffer lacking Mg^{2+} (Figure 7a). In 20 mM KCl assembly occurred with a half-time of 1.7 min for myosin at 2.2×10^{-7} M. At 50 mM K^+ the overall rate dropped approximately 2-fold ($t_{1/2} = 3.5$ min), while at 100 mM K^+ assembly the rate dropped 7.5-fold ($t_{1/2} = 12.8$ min). Since intracellular K^+ in *Dictyostelium* is known to vary within this concentration range in response to cAMP intercellular signaling (Aeckerle et al., 1985), K^+ may influence the rate of cytoplasmic myosin assembly. Inspection of early assembly time points (Figure 7b) disclosed that 20−100 mM K^+ affected only the growth phase of thick filament formation, with rates of nucleation remaining constant. Physiologic K^+ therefore appeared to exert significant inhibitory effects on additions to tetrameric nuclei.

Assembly Acceleration by $MgCl_2$. To determine if any stages of assembly were regulated by Mg^{2+}, assembly was performed in DdM buffer containing 50 mM K^+ and varying concentrations of $MgCl_2$ (Figure 8). Biphasic kinetics were still obtained in 0.1 mM and 1.0 mM $MgCl_2$, but the initial

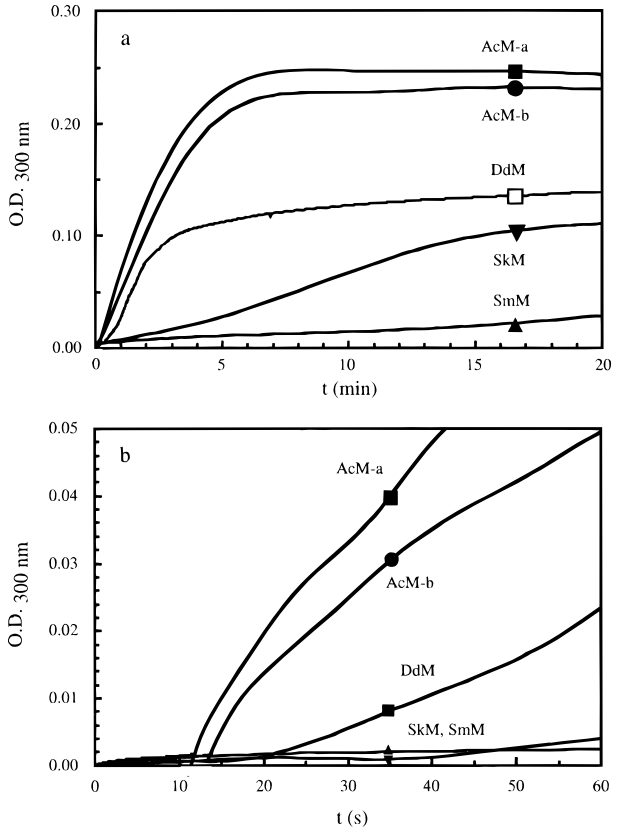

FIGURE 6: Buffer effects on myosin assembly rate. Assembly of 0.22 μM *Dictyostelium* myosin II in buffers conventionally used for analysis of *Acanthamoeba* myosin II (AcM-a and AcM-b), rabbit skeletal muscle myosin (SkM), smooth muscle myosin (SmM), and *Dictyostelium* myosin II (DdM). Representative assembly light-scattering tracings are shown. The initial time courses for assembly curves are depicted. AcM-a (■), AcM-b (●), DdM (□), SkM (▽), SmM (▲).

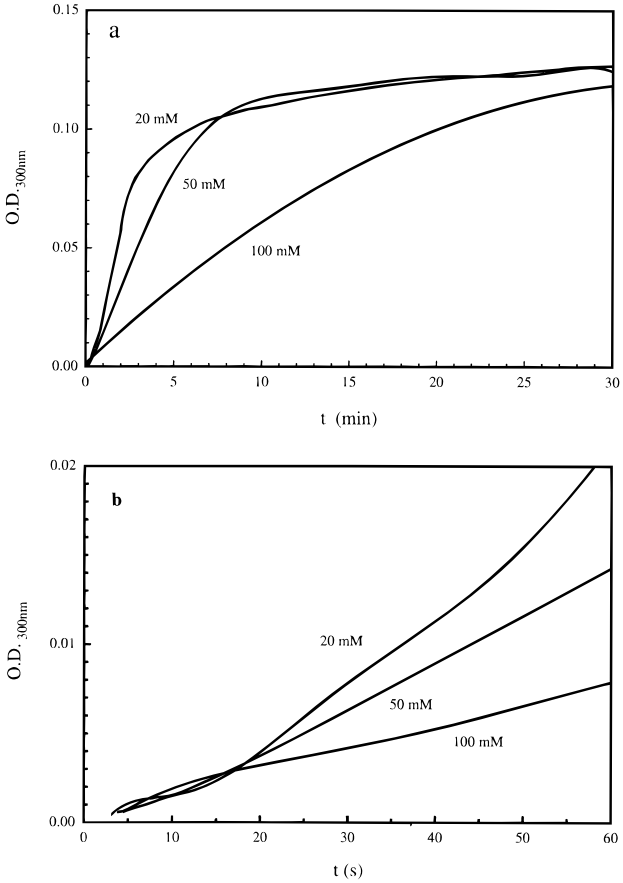

FIGURE 7: Inhibition of myosin assembly by KCl. (a) Representative light-scattering curves for assembly in DdM buffer with varying KCl concentrations. (b) Expanded time course over the initial 60 s of assembly. Increasing KCl from 20 to 100 mM specifically slowed the post-nucleation growth phase of assembly.

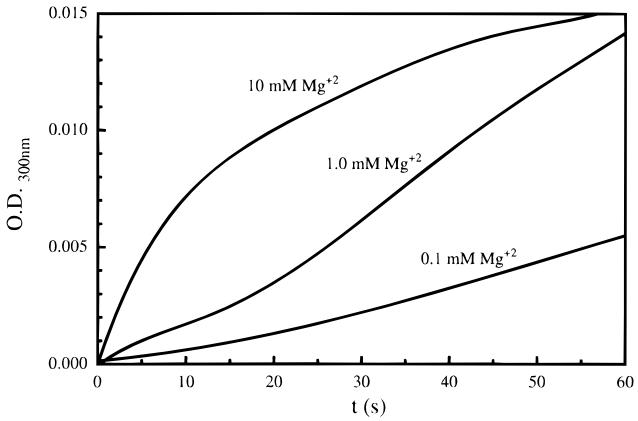

FIGURE 8: Acceleration of assembly nucleation by $MgCl_2$. Light-scattering assembly curves carried out in DdM Buffer containing 0.1, 1.0, and 10 mM $MgCl_2$. Mg^{2+} stimulated the nucleation stage of myosin II assembly.

nucleation phase of the reaction was significantly accelerated by increased Mg^{2+}. At 1.0 mM Mg^{2+} the nucleation rate was approximately 3-fold faster than in 0.1 mM Mg^{2+}. In 10 mM Mg^{2+} a distinct nucleation lag phase was not detected, since assembly was nucleated 11-fold faster than in 0.1 mM Mg^{2+}. In addition, 10 mM Mg^{2+} promoted lateral association of myosin onto nuclei during the later stages of assembly (Figure 6, 120 s), leading to larger diameter thick filaments. These effects can be explained by a single mechanism in which Mg^{2+} enhances lateral associations of myosin monomers into parallel dimers and dimers onto preformed nuclei. Dimer addition to nuclei or thick filaments, however, is competitively inhibited by K^+.

Regulation of Myosin Assembly by F-Actin. Actin filament networks have been shown to accelerate the *in vitro* assembly rate of *Dictyostelium* and smooth muscle myosins (Mahajan et al., 1989; Applegate & Pardee, 1992). Acceleration is mediated by an initial association of myosin monomers with actin filaments. To determine which stage of myosin assembly was regulated by actin filaments, assembly was carried out in the presence of rabbit skeletal muscle F-actin (Figure 9). Control assays with myosin alone in 1 mM ATP showed typical biphasic assembly kinetics with slow nucleation rates. Addition of a 10-fold molar excess of F-actin to myosin monomers in the presence of 1 mM ATP accelerated the inital rate of assembly approximately 25-fold, abolishing the lag phase. Myosin assembled in F-actin and 1 mM AMPPNP showed a 9-fold acceleration of assembly. In F-actin plus 1 mM ADP assembly did not occur due to immediate tight binding of myosin monomers to actin filaments [data not shown; see Mahajan et al. (1989)]. The results support the hypothesis that networks of actin filaments promote initial self-association of myosin monomers during nucleation. Acceleration presumably occurs by an enhanced collision frequency between myosin monomers as they diffuse or slide along actin filaments. In AMPPNP, monomers concentrate about actin filaments due to weak actomyosin associations, while in the presence of ATP, active

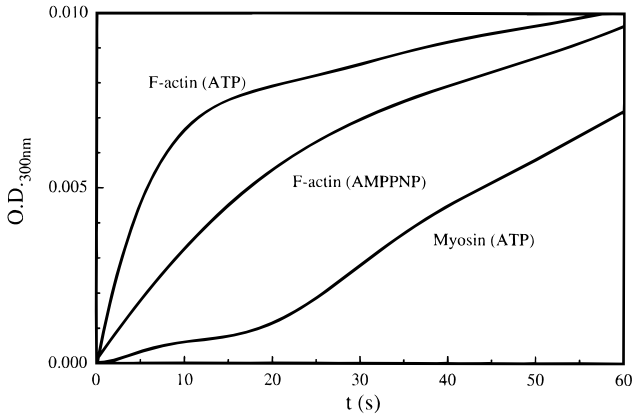

FIGURE 9: Acceleration of myosin assembly by actin filaments. Comparison of *Dictyostelium* myosin II assembly kinetics in the presence or absence of a 10:1 molar ratio of skeletal muscle F-actin. Assembly in the presence of 0.22 μM myosin + 1 mM ATP (myosin ATP), 0.22 μM myosin + 2 μM F-actin + 1 mM AMPPNP (F-actin AMPPNP), and 0.22 μM myosin + 2 μM F-actin + 1 mM ATP (F-actin ATP) are shown. Actin filaments accelerated the nucleation stage of myosin assembly. Assembly curves were corrected for base line light scattering of F-actin in ATP or AMPPNP.

motility of myosin molecules along actin filament networks promotes monomer interactions.

DISCUSSION

Assembly Pathway. On the basis of assembly kinetics and the morphology of intermediates, a two-stage regulated pathway for self-association of *Dictyostelium* myosin II into thick filaments is presented (Figure 10). In physiologic concentrations of K^+, Mg^{2+}, and H_3O^+, myosin monomers initially form parallel dimers that associate into antiparallel tetramers in rate-limiting steps that kinetically define the nucleation stage of assembly. A subsequent growth stage consisting of lateral additions of myosin dimers to the bipolar tetramer template produces thick filaments. Consistent with the view of dimer and tetramer intermediates in the assembly pathway, Pasternack et al. (1989) and Kuczmarski et al. (1987) have observed that *Dictyostelium* myosin II thick filaments are dissociated by low ionic strength buffers into parallel dimers and antiparallel tetramers consisting of dimers joined end-to-end.

Comparative Assembly Properties. The striking kinetic features of *Dictyostelium* myosin II assembly are (i) a clearly defined rate-limiting nucleation stage, (ii) slow assembly kinetics compared to other myosins, and (iii) high sensitivity to inhibition by monovalent ions. Sensitivity to K^+ suggests that fluctuations in cytoplasmic K^+ in *Dictyostelium* (Aeckerle et al., 1985) are sufficient to influence the assembly state of myosin. Assembly of 2×10^{-7} M *Dictyostelium* myosin in 50 mM KCl ($t_{1/2} = 120$ s) was 20 times slower than an equivalent concentration of rabbit skeletal muscle myosin assembled in 180 mM KCl ($t_{1/2} = 5.2$ s; Katsura & Noda, 1973). The pseudo-second-order rate constant of 3.3×10^5 M^{-1} s^{-1} for elongation of rabbit skeletal muscle myosin (Davis, 1981b) is 13-fold faster than the 2.5×10^4 M^{-1} s^{-1} second-order constant of *Dictyostelium* myosin II. None of the buffer conditions tested produced the extremely rapid assembly rate ($k_{obs} > 10^8$ M^{-1} s^{-1}) observed for *Acanthamoeba* myosin II minifilament formation (Sinard & Pollard, 1989). Under AcM-a Buffer conditions that resulted in minifilament formation with *Acanthamoeba* myosin II in milliseconds, *Dictyostelium* myosin II formed antiparallel thick filaments with a $t_{1/2}$ of 100 s. The unmistakable variation in kinetics and structural intermediates formed during nucleation [compare Figure 5 with Sinard et al. (1989)] argues for markedly different assembly mechanisms between these two non-muscle myosins.

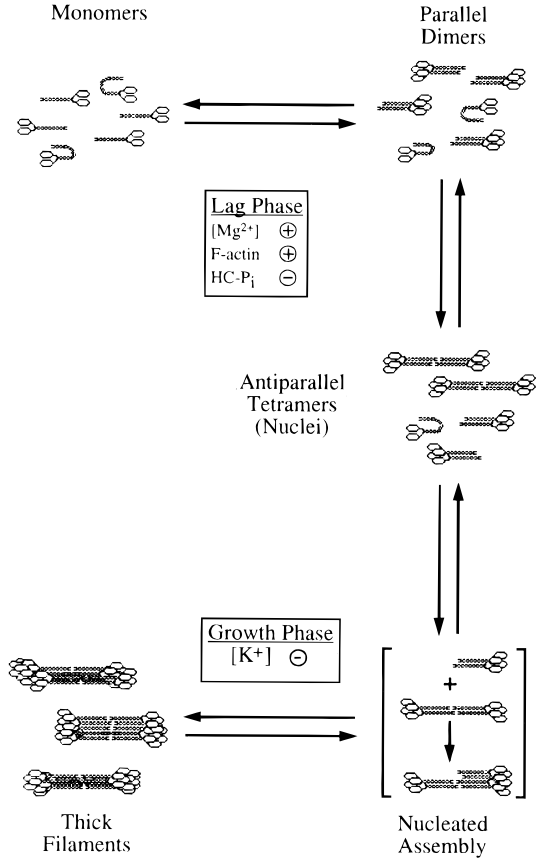

FIGURE 10: Structural stages of *Dictyostelium* myosin II assembly. *Dictyostelium* myosin thick filament formation proceeds in two distinct stages. An initial nucleation step occurs by sequential association of myosin monomers into parallel dimers and antiparallel tetramers. Nucleation is positively regulated by Mg^{2+} and F-actin and is inhibited by myosin tail phosphorylation (HC-P_i). Bent myosin monomers represent heavy chain phosphorylation. Mature thick filaments form by rapid lateral addition of myosin dimers to bipolar nuclei. The growth phase is inhibited by KCl.

Assembly of *Dictyostelium* myosin II incorporates some assembly features previously described for skeletal myosin (Davis, 1985, 1988), including parallel dimer formation during nucleation (Davis et al., 1982), but mechanisms differ during growth off nuclei. While skeletal muscle myosin dimers build a staggered array along bipolar nuclei, *Dictyostelium* myosin II dimers add laterally. As a result, striated muscle thick filaments are long (1.5 μm) and tapered, while *Dictyostelium* filaments are short (0.45 μm) and blunt. Regarding the relationship between turbidity and thick filament growth, Davis (1981a) experimentally determined that a direct measure of the amount of myosin dimer into thick filaments could be obtained by turbidity measurements following partial pressure-jump dissociation of fully assembled thick filaments. The elongation phase of skeletal muscle myosin assembly followed pseudo-second-order kinetics due to a diminishing affinity of dimers for the elongating thick filament. The observed rate constant for skeletal myosin assembly was therefore inversely dependent

on filament concentration (Davis, 1981b). In the work reported here turbidity also showed a linear increase for dimer incorporation into thick filaments of a constant length approximating bipolar tetramers. *Dictyostelium* filament formation followed a strictly second-order kinetic scheme, since k_{obs} for filament growth did not vary with myosin concentration (data not shown). This is consistent with the proposed reaction mechanism of lateral association of myosin dimers into thick filaments with no elongation and no dependence of reaction rate on available thick filament ends. Symmetrical accretion of dimers onto blunt-ended filaments requires only the presence of tetrameric nuclei and a pool of free dimers, the final filament thickness being dependent on the ratio of nuclei and dimers present during nucleation. Thicker diameter filaments assembled in 10 mM Mg^{2+} results from accelerated dimer additions to relatively few nuclei. Monovalent ion concentration also regulates filament thickness by modulating dimer affinity to nuclei. *Acanthamoeba* myosin II utilizes an assembly scheme that proceeds from monomers to antiparallel dimers to antiparallel minifilaments containing staggered arrays of dimers (Sinard et al., 1989), and smooth muscle myosin follows yet another mechanism that incorporates antiparallel dimers into side polar filaments [Atkinson & Stewart, 1992; Cross et al., 1991a,b; reviewed in Trybus (1991)]. With the inclusion of *Dictyostelium*, each conventional myosin examined to date forms bipolar thick filaments through a unique pathway. Diverse assembly regulatory mechanisms appear to be the rule for members of the myosin II family.

Preferred assembly pathways derive primarily from myosin monomer structure. Structural variations between myosins include tail length, carboxy-terminal sequence, rod phosphorylation sites, and light chain phosphorylation, all of which are regulators of assembly and thick filament morphology [Atkinson & Stewart, 1992; Collins et al., 1982; Egelhoff et al., 1993; Faruqi et al., 1993; Hodge et al., 1992; Katsura & Noda, 1971; Kuznicki et al., 1985; McLachlan & Karn, 1982, 1983; Pollard, 1982; Reisler et al., 1980; Suzuki et al., 1982; Trybus & Lowey, 1987; Harrington & Burke, 1972; Hinssen et al., 1978; reviewed in Harrington and Rogers (1984), Korn and Hammer (1988), Trybus (1991), and Warrick and Spudich (1987)]. Structural differences in rod length and structure predict heterogeneous mechanisms of assembly and unique regulation of thick filament, actin interactions. The long-tailed myosin of *Dictyostelium* (170 nm) appears to grow thick filaments by a mechanism similar to that of muscle myosin (150 nm) that maximizes tail overlap of dimers (Godfrey & Harrington, 1970a,b; Harrington & Burke, 1972; Herbert & Carlson, 1971; McLachlan & Karn, 1982, 1983). While end-to-end association of dimers to form tetramers is not highly favorable due to limited C-terminal tail overlap, successive additions of dimers to nuclei would stabilize a bipolar structure. Divergence in tail structure between *Dictyostelium* and muscle myosins has shifted the overlap pattern of dimers onto nuclei to give rise to elongated muscle thick filaments.

Phosphorylation Effects. Tail phosphorylation of *Dictyostelium* myosin has been shown to be a major regulator of assembly (Kuczmarski & Spudich, 1980) and cell phenotype. Cells expressing a myosin II lacking the phosphorylated domain of the tail (DeLozanne & Spudich, 1987) behave like myosin null mutants (Manstein et al., 1989). Tail phosphorylation creates a hairpin loop of the rod, effectively excluding monomers from the assembly pathway under physiologic buffer conditions (Kuczmarski et al., 1987; Pasternak et al., 1989). Dephosphorylation straightens the monomer tail, permitting entry into the assembly pathway. Structures formed by dephosphorylated myosin are identical to those of nonphosphorylated myosin, being limited to parallel dimers and antiparallel tetramers (Kuczmarski et al., 1989; Pasternak et al., 1989). The final forms of thick filaments assembled after tail dephosphorylation match the final assembly states observed in our study. Reversible light chain phosphorylation also results in formation of thick filaments that are indistinguishable from nonphosphorylated *Dictyostelium* myosin II (Griffith et al., 1987). Consequently, dephosphorylated myosin appears to behave identically to nonphosphorylated myosin with respect to the final thick filament product formed. With identical intermediate and thick filament structures, the assembly mechanism presented here applies to both unphosphorylated and dephosphorylated myosin II. Kinetic regulation by phosphorylation therefore reduces to a description of the rate of monomer dephosphorylation by myosin phosphatases. Heavy chain phosphatases specific for myosin have been partially purified from *Dictyostelium* (Kuczmarski & Pagone, 1985) that remove >95% of the phosphate from both the heavy and light chains (Kuczmarski et al., 1987), making possible a kinetic characterization of coupling between monomer dephosphorylation and assembly.

Actin-Accelerated Assembly. We previously reported that actin filament networks accelerate the *in vitro* assembly rate of *Dictyostelium* myosin II (Mahajan et al., 1989). Fluorescence energy transfer indicated that actin-mediated acceleration of myosin assembly occured through an early, nucleotide-dependent interaction of myosin monomers with the actin filaments. As shown here, actin filaments promote myosin assembly by significantly accelerating the rate-limiting nucleation phase of the reaction. Transient binding of myosin along actin filaments presumably concentrates and aligns dimers, accelerating initial tetramer formation. Since *Dictyostelium* myosin II thick filaments are enmeshed in cytoplasmic actin filament networks (Aguado-Velasco & Kuczmarski, 1993; Fukui & Yumura, 1986; Moncman et al., 1993; Yumura & Fukui, 1985), F-actin is likely to play a significant regulatory role in myosin assembly.

ACKNOWLEDGMENT

We gratefully thank Julie A. Johns for expert assistance in electron microscopy of the early time points of myosin assembly.

REFERENCES

Aeckerle, S., Wurster, B., & Malchow, D. (1985) *EMBO J. 4*, 39−43.
Applegate, D., & Pardee, J. D. (1992) *J. Cell Biol. 117*, 1223−1230.
Aguado-Velasco, C., & Kuczmarski, E. R. (1993) *Cell Motil. Cytoskeleton 26*, 103−114.
Atkinson, S. J., & Stewart, M. (1992) *J. Mol. Biol. 226*, 7−13.
Berne, B. J. (1974) *J. Mol. Biol. 89*, 755−758.
Clarke, M., & Spudich, J. A. (1974) *J. Mol. Biol. 86*, 209−222.
Collins, J. H., Cote, G. P., & Korn, E. D. (1982) *J. Biol. Chem. 257*, 4529−4534.
Craig, R., & Megerman, J. (1977) *J. Cell Biol. 75*, 990−996.
Craig, R., Smith, R., & Kendrick-Jones, J. (1983) *Nature 302*, 436−439.

Cross, R. A., Greeves, M. A., & Kendrick-Jones, J. (1991a) *EMBO J. 10*, 747−756.
Cross, R. A., Hodge, T. P., & Kendrick-Jones, J. (1991b) *J. Cell Sci. 14*, 17−21.
Davis, J. S. (1981a) *Biochem. J. 197*, 301−308.
Davis, J. S. (1981b) *Biochem. J. 197*, 309−314.
Davis, J. S. (1985) *Biochemistry 24*, 5263−5269.
Davis, J. S. (1986) *Biophys. J. 50*, 417−422.
Davis, J. S. (1988) *Annu. Rev. Biophys. Biophys. Chem. 17*, 217−239.
Davis, J. S., Buck, J., & Greene, E. P. (1982) *FEBS Lett. 140*, 293−297.
DeLozanne, A., & Spudich, J. A. (1987) *Science* 236, 1086−1091.
Egelhoff, T. T., Lee, R. J., & Spudich, J. A. (1993) *Cell 75*, 363−371.
Faruqi, A. R., Cross, R. A., & Kendrick-Jones, J. (1993) *Adv. Exp. Med. Biol. 332*, 81−89.
Fechheimer, M., & Taylor, D. L. (1984) *J. Biol. Chem. 259*, 4514−4520.
Fechheimer, M., Denny, C., Murphy, R. F., & Taylor, D. L. (1986) *Eur. J. Cell Biol. 40*, 242−247.
Fukui, Y., & Yumura, S. (1986) *Cell Motil. Cytoskeleton 6*, 662−673.
Godfrey, J. E., & Harrington, W. F. (1970a) *Biochemistry 9*, 886−893.
Godfrey, T. E., & Harrington, W. F. (1970b) *Biochemistry 9*, 894−908.
Griffith, L. M., Downs, S. M., & Spudich, J. A. (1987) *J. Cell Biol. 104*, 1309−1323.
Gutfreund, H. (1972) in *Enzymes: Physical Principles*, John Wiley & Sons Ltd., London.
Harrington, W. F., & Burke, M. (1972) *Biochemistry 11*, 1448−1455.
Harrington, W. F., & Rodgers, M. E. (1984) *Annu. Rev. Biochem. 53*, 35−73.
Herbert, T. J., & Carlson, F. D. (1971) *Biopolymers 10*, 2231−2252.
Hinssen, H., D'Haese, J., Small, J. V., & Sobieszek, A. (1978) *J. Ultrastruct. Res. 64*, 282−302.
Hodge, T. P., Cross, R., & Kendrick-Jones, J. (1992) *J. Cell Biol. 118*, 1085−1095.
Johns, J. A., Brock, A. M., & Pardee, J. D. (1988) *Cell Motil. Cytoskeleton 9*, 205−218.
Katsura, I., & Noda, H. H. (1971) *J. Biochem. 69*, 219−229.
Katsura, I., & Noda, H. H. (1973) *Adv. Biophys. 5*, 177−202.
Kendrick-Jones, J., Tooth, P., Taylor, K. A., & Scholey, J. M. (1982). *Cold Spring Harbor Symp. Quant. Biol. 46*, 929−938.
Kitanishi-Yumura, T., & Fukui, Y. (1989) *Cell Motil. Cytoskeleton 12*, 78−89.
Koretz, J. F. (1982) *Methods Enzymol. 85*, 20−55.
Korn, E. D., & Hammer, J. A. (1988) *Annu. Rev. Biophys. Biophys. Chem. 17*, 23−45.
Kuczmarski, E. R., & Spudich, J. A. (1980) *Proc. Natl. Acad. Sci. U.S.A. 77*, 7292−7296.
Kuczmarski, E. R., & Pagone, J. (1985) *J. Muscle Res. Cell Motil. 7*, 501−509.
Kuczmarski, E. R., Tafuri, S. R., & Parysek, L. M. (1987) *J. Cell Biol. 105*, 2989−2997.
Kuczmarski, E. R., Routsolias, L., & Parysek, L. M. (1988) *Cell Motil. Cyotskeleton 10*, 471−481.
Kuznicki, J., Cote, G. P., Bowers, B., & Korn, E. D. (1985) *J. Biol. Chem. 260*, 1967−1972.
Loomis, W. F. (1971) *Exp. Cell Res. 64*, 484−486.
Mahajan, R. K., Vaughan, K. T., Johns, J. A., & Pardee, J. D. (1989) *Proc. Natl. Acad. Sci. U.S.A. 86*, 6161−6165.
Manstein, D. J., Titus, M. A., DeLozanne, A., & Spudich, J. A. (1989) *EMBO J. 8*, 923−932.
Marshall, A. G. (1978) in *Biophysical Chemistry: Principles, Techniques, and Applications*, John Wiley & Sons, New York.
McLachlan, A. D., & Karn, J. (1982) *Nature 299*, 226−231.
McLachlan, A. D., & Karn, J. (1983) *J. Mol. Biol. 164*, 605−626.
Megerman, J., & Lowey, S. (1981) *Biochemistry 20*, 2099−2110.
Moncman, C. L., Rindt, H., Robbins, J., & Winkelmann, D. A. (1993) *Mol. Biol. Cell. 4*, 1051.
Nachmias, V. T., Fukui, Y., & Spudich, J. (1989) *Cell Motil. Cytoskeleton 13*, 158−169.
Oosawa, F., & Kasai, M. (1971) in *Subunits in Biological Systems, Part A* (Timasheff, S. N., & Fasman, G. D., Eds.) pp 261−322, Marcel Dekker, Inc., New York.
Pasternak, C., Flicker, P., Ravid, F. S., & Spudich, J. A. (1989) *J. Cell Biol. 109*, 203−210.
Pepe, F. A. (1982) in *Cell and Muscle Motility* (Dowben, R. M., & Shay, J. W., Eds.) pp 141−177, Plenum Publishing Corp., New York.
Pepe, F. A., & Drucker, B. (1979) *J. Mol. Biol. 130*, 379−393.
Pinset-Harstrom, I., & Truffy, J. (1979) *J. Mol. Biol. 134*, 173−188.
Pollard, T. D. (1982) *J. Cell Biol. 95*, 816−825.
Reisler, E., Smith, C., & Seegan, G. (1980) *J. Mol. Biol. 143*, 129−145.
Reisler, E., Cheung, P., Borochov, N., & Lake, J. A. (1986) *Biochemistry 25*, 326−332.
Saad, A. D., Pardee, J. D., & Fischman, D. A. (1986) *Proc. Natl. Acad. Sci. U.S.A. 83*, 9483−9487.
Sinard, J. H., & Pollard, T. D. (1989) *J. Cell Biol. 109*, 1529−1535.
Sinard, J. H., & Pollard, T. D. (1990) *J. Biol. Chem. 265*, 3654−3660.
Sinard, J. H., Stafford, W. F., & Pollard, T. D. (1989) *J. Cell Biol. 109*, 1537−1547.
Small, J. V., & Sobieszek, A. (1980) *Int. Rev. Cytol. 64*, 241−306.
Spudich, J. A. (1982) *Methods Cell Biol. 25*, 359−364.
Stewart, P. R., & Spudich, J. A. (1979) *J. Supramol. Struct. 12*, 1−14.
Suzuki, H., Takahashi, K., Onishi, H., & Watanabe, S. (1982) *J. Biochem. 91*, 1687−1698.
Trybus, K. M. (1991) *Curr. Opin. Cell Biol. 3*, 105−111.
Trybus, K. M., & Lowey, S. (1987) *J. Cell Biol. 105*, 3007−3019.
Warrick, H. M., & Spudich, J. A. (1987) *Annu. Rev. Cell Biol. 3*, 379−421.
Yumura, S., & Fukui, Y. (1985) *Nature 314*, 194−196.

BI9618981